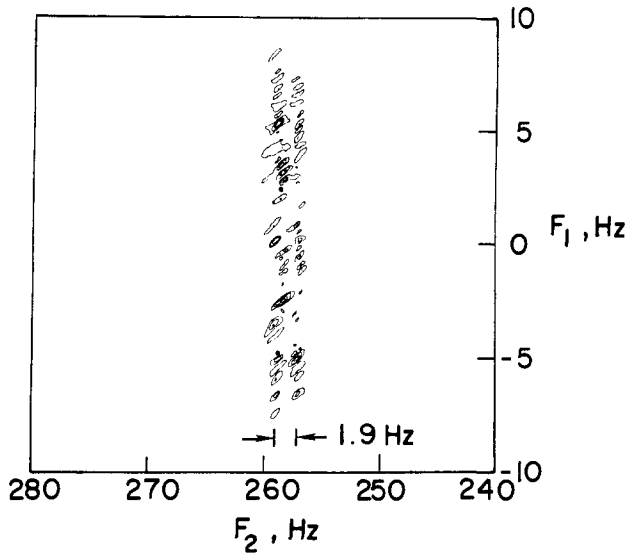

Figure 3. Two-dimensional contour plot associated with the H4 proton of 1-fluorobicyclo[2.2.1]heptane. The interproton coupling constants occur along the F_1 axis, and the $^1H-^{19}F$ coupling constant is measured along the F_2 axis. The center of this doublet corresponds to δ 2.08.

mensional FT NMR technique[24] was used to obtain the $^1H-^{13}C$ and $^1H-^{19}F$ coupling constants. The data were collected by the Hahn spin-echo pulse sequence[25] using a 16-phase cycle[26] to cancel pulse errors. The 90° pulse-τ-180° pulse-data acquisition period-recovery period used τ values from 0.01 to 1.42 s, incremented in units of 0.0111 s to give spectral widths of +22.52 to -22.52 Hz along the F_1 axis. The recovery period was at least 8 s to prevent the formation of spurious peaks. The usual F_2 spectral width was 360 Hz, which was collected into a 2K word file with an acquisition time of 2.84 s. After zero-filling along both the F_1 and F_2 axes, the digital resolution was 0.18 Hz per point. The total data collection times for the two-dimensional spectra were 42 h. The data were manipulated with Bruker Instruments' FTNMR 2D computer program.[27] After a 45° tilt of the two-dimensional data, the contour plots of the bridgehead hydrogens showed the complicated splitting pattern due to the interproton coupling along the F_1 axis, and the coupling to the heteroatoms is given along the F_2 or chemical shift axis. A simplified diagram of the type of data obtained by this two-dimensional technique applied to 1-fluorobicyclo[2.2.1]heptane (**2d**) is given in the contour plot of Figure 3. The bridgehead proton produces a very complicated splitting pattern as two vertical rows of peaks along F_1 due to coupling to the other ten protons in the molecule. The rows are separated by the long-range $^1H-^{19}F$ coupling constant of 1.9 Hz, which is centered on the chemical shift of the multiplet at δ 2.08.

The coupling constant between the bridgehead hydrogen and the carboxyl ^{13}C in **2b** was found to be less than 0.7 Hz by comparison of the spectra of the labeled and unlabeled compounds. A more refined value of the line width of the bridgehead carbon C4 in the proton-decoupled ^{13}C NMR spectrum of 1-deuteriobicyclo[2.2.2]octane (**1a**) gave a value $J(^1H-^2H) \leq 0.15$ Hz, from which it follows that $J_{CH} < 1$ Hz.

Acknowledgment is made to the donors of the Petroleum Research Fund, administered by the American Chemical Society, for partial support of this research, to the National Science Foundation for assisting in the purchase of the 250-MHz NMR spectrometer, and to the Australian Research Grants Committee. S.R.W. acknowledges the award of the Carl S. Marvel Fellowship for 1980-1981. Services of the University of Arizona Computer Center were essential to the completion of this work.

Registry No. 1a (X = H), 280-33-1; **1b**, 73948-77-3; **1c**, 73948-81-9; **1d**, 20277-22-9; **2a**, 279-23-2; **2b**, 73948-78-4; **2c**, 73948-82-0; **2d**, 78142-52-6; **3a**, 285-86-9; **3b**, 73948-79-5; **3c**, 73948-83-1; **3d**, 78142-55-9; **4a**, 311-75-1; **4b**, 73948-80-8; **4c**, 73948-84-2; **4d**, 78142-58-2; **1a** (X = D), 59346-71-3.

(24) Bodenhausen, G.; Freeman, R.; Niedermeyer, R.; Turner, D. L. *J. Magn. Reson.* **1977**, *26*, 133.
(25) Hahn, E. L. *Phys. Rev.* **1950**, *80*, 580.
(26) Bodenhausen, G.; Freeman, R.; Turner, D. L. *J. Magn. Reson.* **1977**, *27*, 511.
(27) Bruker Instruments, Inc., Manning Park, Billerica, MA 01821.

Electron Spin-Echo Studies of the Solvation Structure of O_2^- in Water

P. A. Narayana, Darbha Suryanarayana, and Larry Kevan*

Contribution from the Department of Chemistry, University of Houston, Houston, Texas 77004. *Received December 28, 1981*

Abstract: The solvation structure of O_2^- in D_2O frozen solutions has been determined with use of electron spin-echo modulation at 4.2 K. The modulation has been analyzed with use of a Fourier transformation technique combined with direct simulation of the modulation. The analysis indicates that the first solvation shell waters have an H-O bond dipole orientation toward O_2^- and that each O_2^- is surrounded by four water molecules. The distance between the center of O_2^- and the nearest deuteron of a water molecule is 0.24 nm and the deuteron has an isotropic coupling of 0.4 MHz, while the distance to the next nearest deuteron on the same water molecule is found to be 0.34 nm. This solvation structure is discussed in terms of probable bonding interactions and is compared with that of solvated electrons in aqueous matrices.

The solvation of the superoxide ion, O_2^-, in bulk solution and on surfaces is of current chemical importance because of (a) the dependence of solvent-molecule orientation on anion size,[1] (b) the existence of O_2^- on catalytic oxide surfaces,[2] and (c) the reactivity of O_2^- in various biological reactions.[3] Thus, we are currently investigating the solvation structure of O_2^- in frozen solutions[4] and on surfaces.[5] This has been made possible by advances in the analysis of electron spin-echo modulation spectrometry.[6] The first study of O_2^- solvation was in frozen solutions of dimethyl sulfoxide.[4] There we showed that the analysis of

(1) Kevan, L. *J. Phys. Chem.* **1981**, *85*, 1628.
(2) Kanazaki, N. I.; Yasumori, I. *Bull. Chem. Soc. Jpn.* **1979**, *52*, 1923.
(3) Fee, J. A.; Valentine, J. S. "Superoxide and Superoxide Dismutase", McCord, J. S., Ed.; Academic Press: New York, 1977.
(4) Narayana, P. A.; Kevan, L. *J. Magn. Reson.* **1982**, *46*, 84.
(5) Narayana, M.; Janakiraman, R.; Kevan, L., unpublished work.
(6) Kevan, L. "Time Domain Electron Spin Resonance", Kevan, L., Schwartz, R. N., Eds.; Wiley-Interscience: New York, 1979; Chapter 8.

0002-7863/82/1504-3552$01.25/0

complex spin-echo modulation is facilitated by employing Fourier transformation together with direct simulation techniques. In this paper we apply this type of analysis to determine the solvation structure of the superoxide ion in frozen aqueous solutions.

Experimental Section

The superoxide ion was produced by dissolving 0.1 mM of K_2O in D_2O (Stohler Isotope Chemicals) and stirring the solution in a nitrogen atmosphere for about 15 min. The resulting solution was quickly frozen to obtain opaque polycrystalline samples. We have also prepared O_2^- in 6 M NaOD which freezes to an aqueous glass.

The spin-echo data were recorded at 4.2 K on a home-built spectrometer.[7] All calculations and simulations were carried out on a Tektronix 4052 graphics system interfaced to a Honeywell 66/60 computer system.

Theory and Analysis

The electron spin-echo modulation was analyzed with use of Fourier transformation and direct simulation techniques. The theory and application of electron spin-echo modulation have been discussed in detail.[6,8] The echo amplitude in the presence of modulation is given by

$$E(\tau') = F_0(\tau')\{1 - \sum_{r=1}^{2n} a_r[1 - F_r(\tau') \cos \omega_r\tau']\} \qquad (1)$$

where $\tau' = \tau + T$, τ and T being the time separations between microwave pulses I and II and II and III, respectively, and the ω_r's being the superhyperfine frequencies. In a two-pulse experiment, $\tau' = \tau$ and the echo intensity is recorded as a function of τ, while in a three-pulse experiment the echo is usually recorded as a function of T. In deriving eq 1 it is assumed that the homogeneous broadening of the nuclear resonance lines is given by the function $F_r(\tau')$ and that all remaining mechanisms that cause the echo decay are represented by the function $F_0(\tau')$. In the absence of the decay $F_0(\tau')$, the Fourier transform of eq 1 yields $2n$ superhyperfine lines and a δ function at the origin. Each of these superhyperfine lines is centered at ω_r with an amplitude a_r and a shape given by the Fourier transform of $F_r(\tau')$. The presence of $F_0(\tau')$ has the effect of broadening these superhyperfine lines and the δ function at the origin in the frequency spectrum, so it is desirable to divide the experimentally recorded data by the decay function. Equation 1 can be rewritten in a slightly different form as[4]

$$E(\tau') = F_0'(\tau')\{[1 + \sum_{r=1}^{2n} a_r'F_r(\tau') \cos \omega_r\tau']\} \qquad (2)$$

where

$$F_0'(\tau') = F_0(\tau')(1 - \sum_r a_r)$$

$$a_r' = a_r(1 - \sum_r a_r)^{-1}$$

Thus in the presence of modulation, the decay function is given by $F_0'(\tau')$. The shape of this function is seldom known. Following the procedure of Blumberg et al.,[9] this function is fitted to a fifth degree polynomial with use of a least-squares routine. Equations 1 and 2 are valid for oriented single crystals. However, for weak electron–nuclear interactions, these equations can be applied for polycrystalline samples also.[4]

A serious problem arises in Fourier transforming the recorded modulation because of the truncation of the recorded echo envelope at short times due to the time response of the spectrometer system. However, this problem can be eliminated to some extent by apodizing the data with an appropriate window function.[10,11] We chose a window function suggested by Bingham et al.[12] which has the following form:

$$h(\tau') = 1 \qquad \text{for } \tau + \Gamma(\tau_f - \tau_i) \le \tau' \le \tau_f - \Gamma(\tau_f - \tau_i')$$

$$h(\tau') = \frac{1}{2}\left[1 - \cos \frac{\pi}{\Gamma} \frac{\tau' - \tau_i}{\tau_f - \tau_i}\right]$$

$$\text{for } \tau_i \le \tau' \le \tau_i + \Gamma(\tau_f - \tau_i)$$

$$h(\tau') = \frac{1}{2}\left[1 - \cos \frac{\pi}{\Gamma} \frac{\tau' - \tau_f}{\tau_f - \tau_i}\right]$$

$$\text{for } \tau_f - \Gamma(\tau_f - \tau_i) \le \tau' \le \tau_f$$

$$h(\tau') = 0 \qquad \text{otherwise}$$

In the above expressions τ_i is the time at which acceptable data starts and τ_f is the time when the recording of data ends. The parameter Γ lies in the range $0 \le \Gamma \le 0.5$. A value of $\Gamma = 0.5$ corresponds to the well-known Hanning Window.[13]

The electron spin-echo modulations were simulated by using the procedure of Narayana et al.[14]

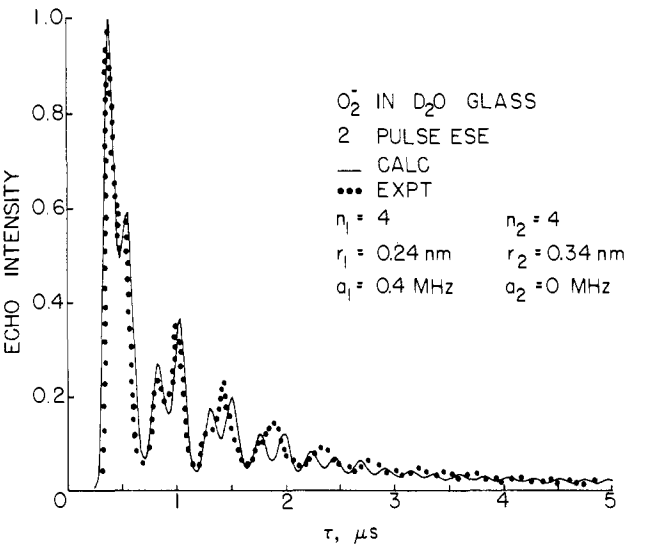

Figure 1. Comparison of the experimental and calculated two-pulse electron spin-echo envelopes for 0.1 mM O_2^- in D_2O glass. The data were recorded at 4.2 K. The parameters used for calculating the deuterium modulation are $n_1 = 4$, $r_1 = 0.24$ nm, and $a_1 = 0.4$ MHz for the first deuterium shell and $n_2 = 4$, $r_2 = 0.34$ nm, and $a_2 = 0$ for the second deuterium shell. The calculated modulation is multiplied by the decay function $\exp(3.33 - 3.17\tau + 1.74\tau^2 - 0.59\tau^3)$ to facilitate direct comparison with the experimental data.

Results

In order to confirm that the paramagnetic species produced is the superoxide ion O_2^-, we have recorded the ESR spectrum at 77 K. The ESR spectrum in polycrystalline ice shows a very broad feature around $g_\parallel = 2.11$ and a strong line at $g_\perp = 2.002$. However, in the aqueous glass, a well-defined peak with $g_\parallel = 2.067$ and a strong line at $g_\perp = 2.002$ are observed. These features are identical with those reported[15] for O_2^-, thus confirming that O_2^- is produced in our aqueous samples.

The two-pulse electron spin-echo of O_2^- in aqueous glass, recorded at 4.2 K, is shown in Figure 1. The echo envelope shows

(7) Ichikawa, T.; Kevan, L.; Narayana, P. A. *J. Phys. Chem.* **1979**, *83*, 3378.
(8) Mims, W. B. "Electron Paramagnetic Resonance", Geschwind, S., Ed.; Plenum: New York, 1972; Chapter 4.
(9) Blumberg, W. E.; Mims, W. B.; Zuckerman, D. *Rev. Sci. Instrum.* **1973**, *44*, 546.
(10) Merks, R. P. J.; deBeer, R. *J. Magn. Reson.* **1980**, *37*, 305.
(11) Aruna, B.; Ramakrishna, Y. V. S.; Narayana, P. A. *Phys. Status Solidi B* **1980**, *101*, 791.
(12) Bingham, C.; Godfrey, M. B.; Tukey, J. W. *IEEE Trans. Audio Electroacoust.* **1967**, *AV15*, 56.
(13) Shaw, D. "Fourier Transform NMR Spectroscopy"; Elsevier: Amsterdam, 1976.
(14) Narayana, P. A.; Bowman, M. K.; Kevan, L.; Yudanov, V. F.; Tsvetkov, Yu. D. *J. Chem. Phys.* **1975**, *63*, 3365.
(15) Symons, M. C. R.; Eastland, G. W.; Denny, L. R. *J. Chem. Soc., Faraday Trans. 1* **1980**, *76*, 1868.

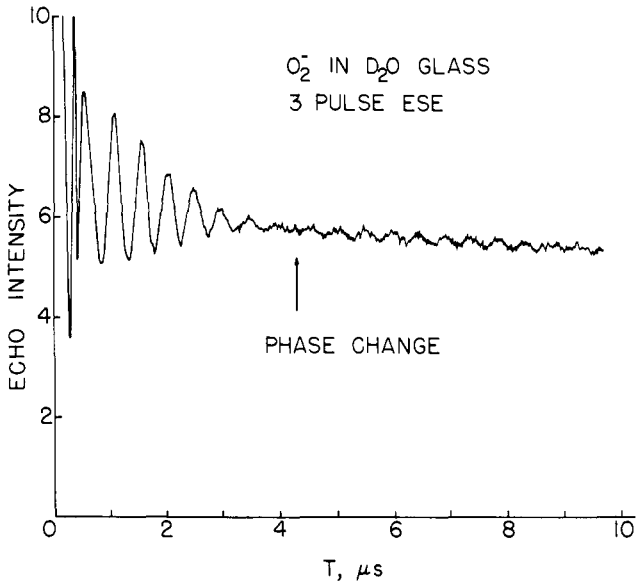

Figure 2. Three-pulse electron spin-echo modulation of 0.1 mM O_2^- in D_2O glass at 4.2 K for $\tau = 0.3$ μs.

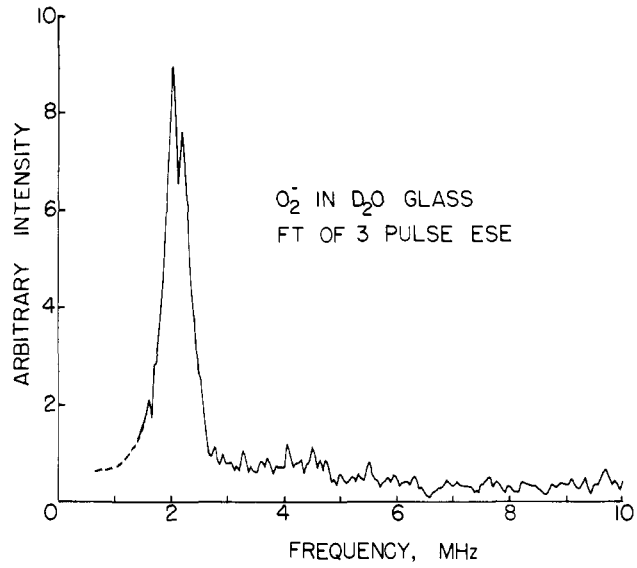

Figure 3. Fourier transformed spectrum of the modulation shown in Figure 2 for O_2^- in D_2O glass. The value of Γ is 0.1. The data were derived by the decay function $\exp(1.955 - 0.31T + 0.09T^2 - 0.01T^3)$.

deep modulation arising from dipolar interaction between O_2^- and the deuterium nuclei of surrounding water molecules. The two-pulse and three-pulse spin-echo envelopes of O_2^- in polycrystalline and glassy ice are virtually identical. We shall therefore refer only to O_2^- in glassy ice. We have also recorded three-pulse electron spin-echoes for various values of τ in the range of 0.3 μs $\leq \tau \leq$ 0.7 μs. A typical three-pulse echo envelope recorded at 4.2 K for $\tau = 0.3$ μs is shown in Figure 2. The envelope also shows deuterium modulation. The interesting feature of this modulation is that it shows phase reversal around 4.2 μs. This observation is important because it can be related to the distance of weakly interacting nuclei.[16]

The observed two-pulse spin-echo modulation very strongly implies the presence of more than one type of interacting deuterium nucleus.[4,14] This is also attested to by the observation of phase reversal in the three-pulse echo modulation. Since the three-pulse echo persists for a longer time, it is more sensitive to weaker interactions. This phase reversal can be related to the distance of the interacting nuclei with the relation[14]

$$r(\text{Å}) = [10.7(T_p + \tau)]^{1/3} \quad (3)$$

where T_p is the time at which phase reversal in the modulation occurs. We have recorded three-pulse echo envelopes for various values of τ in the range $0.3 \leq \tau \leq 0.7$ μs and we have observed phase reversals in the range of 4.0–4.2 μs. When the appropriate values are put into eq 3, we obtain values for r in the range 0.36–0.37 nm. Simulations show that nuclei located at such a distance are too far to give rise to the deep modulation observed in the two-pulse echo envelope. Thus, it is clear that O_2^- also interacts with deuterium nuclei located closer than 0.36 nm. In order to obtain information about the closer nuclei, we have Fourier transformed the three-pulse echo modulation shown in Figure 2 after carrying out the mathematical manipulations described earlier. The Fourier transformed (FT) spectrum is shown in Figure 3. The FT spectrum exhibits a double-peaked line with peaks at 2.0 and 2.2 MHz. The peak at 2.2 MHz corresponds to the free deuterium frequency at the applied magnetic field. The Fourier transformation of three-pulse echo modulations recorded for different values of τ did not reveal the presence of any other frequency components.

Discussion

Both the phase reversal observed in the three-pulse modulation and the observation of two peaks in the FT spectrum clearly confirm the presence of more than one type of interacting deuterium nucleus. The peak at 2.2 MHz in the FT spectrum corresponds to the deuterium Larmor frequency, and therefore it appears that one set of interacting nuclei has zero isotropic hyperfine coupling or nearly so. We identify this with the set of nuclei located around 0.36 nm. The value 0.36 nm is calculated from the position of the observed phase reversal.

In the presence of isotropic hyperfine coupling, one expects to see two peaks at $\omega_I \pm (a/2)$ at large distances where the modulation is fairly regular. Here ω_I is the free nuclear frequency and a is the isotropic hyperfine coupling constant. By Fourier transforming various simulated modulation patterns corresponding to different distances, we find empirically that the "large distance" for deuterium modulation is $\gtrsim$0.33 nm, in which case two peaks at $\omega_I \pm (a/2)$ are calculated. However, for shorter distances only one peak is calculated close to $\omega_I - (a/2)$. This has been discussed earlier.[4] We therefore interpret the peak at 2.0 MHz as arising from closer deuterium nuclei with an isotropic coupling of ~0.4 MHz.

On the basis of these constants, we made a series of two-shell simulations and the best overall fit to the two-pulse modulation was obtained for $n_1 = 4$, $r_1 = 0.24$ nm, and $a_1 = 0.4$ MHz and $n_2 = 4$, $r_2 = 0.34$ nm, and $a_2 = 0$ where subscripts 1 and 2 refer to the two groups of interacting nuclei. To facilitate direct comparison with the experimental modulation, we multiplied the simulated modulation by the decay function $Y = \sum_{i=0}^{3} (\exp(A_i\tau^i)$, where the A_i coefficients are given in the caption of Figure 1. Figure 1 shows that the comparison between the experimental and simulated two-pulse modulation is good. Using the same parameters, we have calculated the Fourier transform spectrum of the three-pulse modulation and find good agreement with Figure 3.

These results suggest that each O_2^- is surrounded by eight deuterons, four arising from each shell. This could correspond to two dipole oriented water molecules in the first shell and two other dipole oriented water molecules in the second shell or to four D–O bond oriented water molecules. We favor the latter model because of better hydrogen bonding interactions; this will be shown to be consistent with the geometry of an individual water molecule. The distance of 0.24 nm then corresponds to the distance between the center of the unpaired electron density in O_2^- and one deuteron of a water molecule, while the distance 0.34 nm corresponds to the distance between O_2^- and the second deuteron of the same water molecule.

In order to propose a particular geometric model, we note that the electronic configuration of O_2^- is π^{*3} and therefore we would have g values of 0 and 4 in the absence of any solvent perturbation. As solvent interactions quench the angular momentum, the values

(16) Narayana, P. A.; Kevan, L. *J. Magn. Reson.* **1976**, *23*, 385.

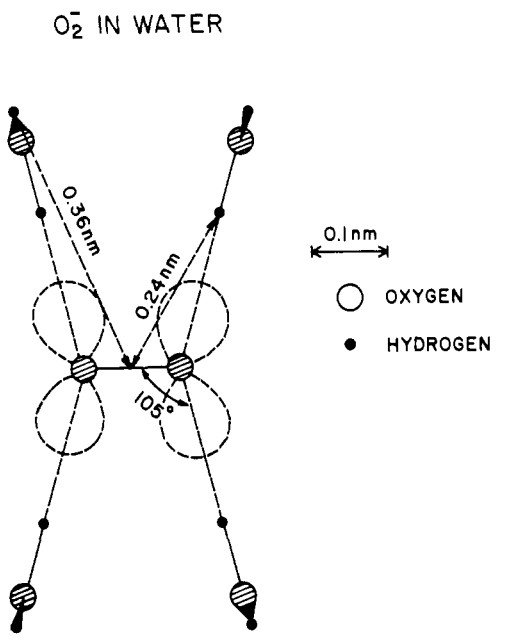

Figure 4. A suggested model for the solvation structure of O_2^- in D_2O. The π^* orbital for the unpaired electron is shown; the O–D bond of each water is approximately oriented toward this orbital to optimize hydrogen bonding. The O_2^- and nearest O–D bonds are coplanar with the other O–D bond alternately perpendicular to this plane as shown.

of $g_{\parallel}$ and $g_{\perp}$ both tend toward 2. It has been suggested that the solvent interaction occurs via hydrogen bonding.[17] Our results, implying an O–D bond orientation for the first solvation shell water molecules, support a hydrogen bonding picture. Maximal hydrogen bonding interaction is achieved by orienting the first solvation shell waters so as to achieve maximum overlap with the orbital containing the unpaired electron. Figure 4 shows such a model. One O–D bond of each water is oriented toward the center of the O–O bond. The other O–D bonds are oriented perpendicular to the plane of O_2^- and the nearest O–D bonds as shown in Figure 4. Then from the nearest neighbor deuteron distance of 0.24 nm, the gas-phase geometry of the water molecules, and 0.126 nm for the bond length of O_2^-, we calculate the distance to the more distant deuteron of the water molecule as 0.36 nm. This is in good agreement with the value of 0.34 nm determined from the spin-echo data.

It is interesting to compare this solvation structure of O_2^- with that of solvated electrons in frozen aqueous glasses.[18,19] In both cases it appears that a bond dipole oriented model is preferred to a molecular dipole oriented model. However, in the case of solvated electrons, there are six first solvation shell molecules arranged approximately octahedrally, while in the case of O_2^- there are four water molecules with the nearest O–D bonds arranged in a planar configuration. In the case of solvated electrons, the ground-state orbital is a spherically symmetric 1s type orbital[20] so that a symmetric arrangement of the first solvation shell molecules is expected. However, in O_2^- the directionality of the unpaired electron π^* orbital predicts a less symmetric arrangement of the first solvation shell molecules.

The ESR spectrum of O_2^- in glassy ice exhibits a well-defined peak at $g_{\parallel} = 2.067$ while O_2^- in polycrystalline ice shows a very broad feature around $g_{\parallel} = 2.11$. This difference has been interpreted that phase separation occurs upon freezing polycrystalline ice to give pure ice regions and concentrated superoxide solution regions.[15] It was concluded that in polycrystalline ice O_2^- does not have a well-defined solvation structure, while O_2^- in glassy ice is characterized by well-defined solvation structure.

Our spin-echo studies show no significant difference between polycrystalline ice and glassy ice. The differences between the ESR and spin-echo observations can be understood as follows. In polycrystalline ice it is assumed that a majority of the O_2^- ions have a well-defined solvation structure identical with those occurring in glassy ice and that a second population of O_2^- exist in regions where the concentration of O_2^- is high and the solvation structure is ill-defined. The dipolar coupling between O_2^- in these latter regions is likely to be strong enough to produce a phase memory time shorter than our detection capability. In this case, the spin-echo envelope of O_2^- in polycrystalline ice would be due only to those superoxide ions with a well-defined solvation structure.

Acknowledgment. This work was supported by the National Science Foundation.

Registry No. Superoxide, 11062-77-4.

(17) Eastland, G. W.; Symons, M. C. R. *J. Phys. Chem.* **1977**, *81*, 1502.

(18) Schlick, S.; Narayana, P. A.; Kevan, L. *J. Chem. Phys.* **1976**, *64*, 3153.

(19) Kevan, L. *Acc. Chem. Res.* **1981**, *14*, 138.

(20) Feng, D. F.; Kevan, L. *Chem. Rev.* **1980**, *80*, 1.